AWARD NUMBER: W81XWH-15-1-0703

TITLE: CXCL14 Blockade of CXCL12/CXCR4 Signaling in Prostate Cancer Bone Metastasis

PRINCIPAL INVESTIGATOR: Gregory A. Clines, MD, PhD

CONTRACTING ORGANIZATION: Regents of the University of Michigan
Ann Arbor, Michigan 48109

REPORT DATE: October 2017

TYPE OF REPORT: Annual

PREPARED FOR: U.S. Army Medical Research and Materiel Command
Fort Detrick, Maryland 21702-5012

REPORT DOCUMENTATION PAGE

Form Approved
OMB No. 0704-0188

1. REPORT DATE	2. REPORT TYPE	3. DATES COVERED
October 2017	Annual	30 Sep 2016 - 29 Sep 2017

4. TITLE AND SUBTITLE

CXCL14 Blockade of CXCL12/CXCR4 Signaling in Prostate Cancer Bone Metastasis

5a. CONTRACT NUMBER

5b. GRANT NUMBER
W81XWH-15-1-0703

5c. PROGRAM ELEMENT NUMBER

6. AUTHOR(S)
Gregory A. Clines, MD, PhD

E-Mail: clines@umich.edu

5d. PROJECT NUMBER

5e. TASK NUMBER

5f. WORK UNIT NUMBER

7. PERFORMING ORGANIZATION NAME(S) AND ADDRESS(ES)

Regents of the University of Michigan
3003 S. State St.
Ann Arbor, Michigan 48109-1274

8. PERFORMING ORGANIZATION REPORT NUMBER

9. SPONSORING / MONITORING AGENCY NAME(S) AND ADDRESS(ES)

U.S. Army Medical Research and Materiel Command
Fort Detrick, Maryland 21702-5012

10. SPONSOR/MONITOR'S ACRONYM(S)

11. SPONSOR/MONITOR'S REPORT NUMBER(S)

12. DISTRIBUTION / AVAILABILITY STATEMENT

Approved for Public Release; Distribution Unlimited

13. SUPPLEMENTARY NOTES

14. ABSTRACT

Bone metastasis is a common and unfortunate complication of advanced prostate cancer resulting in significant pain and fractures. The most devastating consequence, however, is that once the cancer has metastasized to bone, the disease is incurable. Up to 90% of men who succumb to prostate cancer have bone metastasis, which demonstrates the strong attraction of prostate cancer to bone. Chemokines are essential in cancer progression and metastasis. The chemokine CXCL14 was identified in a screen for factors that support prostate cancer bone metastasis. In a human prostate cancer tissue microarray, CXCL14 expression was found significantly greater in prostate cancer metastasis to bone compared to metastasis to other organs, suggesting that this chemokine has important effects that are specific to bone. The goal of this proposal is to understand the role of CXCL14 in the homing and progression of prostate cancer to bone.

15. SUBJECT TERMS
Prostate cancer, bone metastasis, CXCL14, chemokine signaling, animal models

16. SECURITY CLASSIFICATION OF:			17. LIMITATION OF ABSTRACT	18. NUMBER OF PAGES	19a. NAME OF RESPONSIBLE PERSON
a. REPORT	b. ABSTRACT	c. THIS PAGE			USAMRMC
U	U	U	UU	57	19b. TELEPHONE NUMBER *(include area code)*

Table of Contents

Page

1. Introduction

Chemokines play critical roles in cancer progression and metastasis. We identified the chemokine CXCL14 in a screen of factors expressed in prostate cancer bone metastasis. In a human prostate cancer tissue microarray, CXCL14 expression was significantly greater in metastasis to bone compared to soft tissue metastasis, primary prostate tumors and normal prostate. CXCL14 expression was also significantly greater in bone xenografts compared to growth outside the skeleton in animal models of bone metastasis. These data suggest bone-specific actions of prostate cancer and CXCL14. The purpose of this proposal is to understand the role of CXCL14 in the development and progression of prostate cancer bone metastasis.

2. Keywords

Prostate cancer, bone metastasis, CXCL14, chemokine signaling, animal models

3. Accomplishments

Major goals:

1. Assess prostate cancer CXCL14 overexpression to reduce CXCL12-mediated homing to bone
2. Assess the effects of CXCL14 knockdown to reduce prostate cancer growth in bone

Accomplishments

1. A manuscript has been submitted detailing the molecular actions of CXCL14 on prostate cancer cells. The receptor for CXCL14 had not been clearly defined in the past and controversy existed as to the extent to which CXCR4 acted as the receptor. We have new data showing that CXCL14 does not directly interact with CXCR4, but CXCR4 is dependent on at least some of CXCL14 cellular actions. These data suggest, as has been reported previously, that CXCR4 likely exists as a heterodimer with the unidentified CXCL14 receptor. A manuscript submitted to the journal *Oncotarget* is attached in the Appendix.
2. Using prostate cancer PC-3 cells that overexpress luciferase, we have generated these PC-3 cells to overexpress CXCL14 versus an empty vector control. After intracardiac inoculation, the development of bone and soft tissue lesions was monitored using *in vivo* bioluminescent imaging. This experiment recently ended, 13 weeks after intracardiac inoculation. An example of the same lesion as seen by X-ray and IVIS is shown (Figure). Analyses examining for differences in percent of mice with bone lesions by X-ray, percent of mice with bone lesions on X-ray + IVIS imaging, average number of lesions/mice on X-ray, and average number of lesions on X-ray + IVIS imaging was not different (Figure).

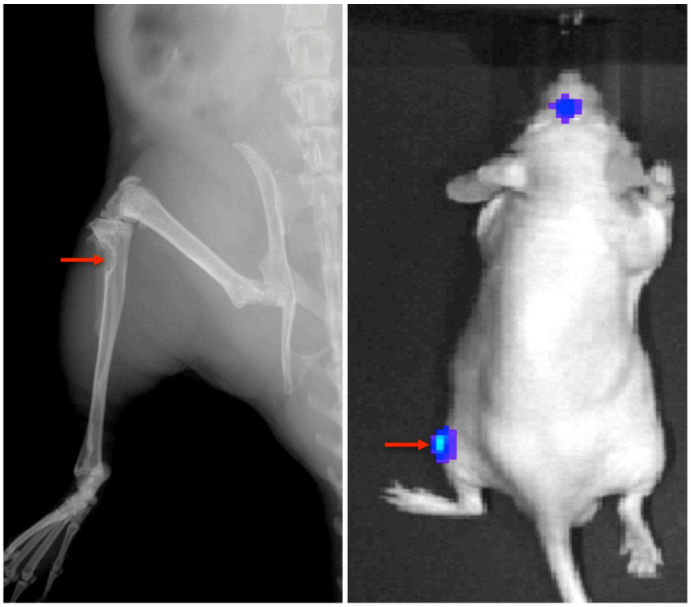

	Empty Vector	CXCL14	p-value
Percent of Mice with Lesions on X-ray	55%	27%	0.2049
Percent of Mice with Lesions/Signals on X-ray/IVIS	67%	45%	0.3110
Average Number of Lesions per Mouse on X-ray (Mean ± SEM)	0.6667 ± 0.2357	0.4545 ± 0.2817	0.5815
Average Number of Lesions/Signals on X-ray/IVIS (Mean ± SEM)	1.333 ± 0.4082	1.273 ± 0.5062	0.9291

Opportunities for training and professional development
Nothing to report

Dissemination of results to the communities of interest
The publication entitled “CXCL14 is a Pro-Metastatic Chemokine with CXCR4 Dependent and Independent Actions” was submitted to the Journal Oncotarget. A decision of “Accept Pending Major Revisions” was made, and this paper is currently being revised.

Plans during the next reporting period
We will begin work on the following:

Task 1b: Examine competition of CXCL12 and CXCL14 in prostate cancer skeletal invasion. Based on new data, we will change the approach of this task. See details below.
Task 2a: Examine how CXCL14 knockdown in prostate cancer cells, before the arrival to bone, affects the development of bone lesions in a bone metastasis prevention model

4. Impact

Impact on the development of the principal discipline of the project

1. Our recent results confirm that CXCL14 signaling is more complex that once thought and likely involves an unidentified CXCL14 chemokine receptor cooperating with CXCR4.
2. The original hypothesis that CXCL14 is a CXCL12 inhibitor has been modified so that CXCL14 likely has cooperative actions with CXCL12 in prostate cancer bone metastasis.

Impact on other disciplines
Nothing to report

Impact on technology transfer
Nothing to report

Impact on society beyond science and technology
Nothing to report

5. Changes/Problems

Changes in approach and reasons for change
Based on our preliminary data and hypothesis that CXCL12 and CXCL14 compete for the same receptor, we have new data that this is not the case. As reported in the attached submitted manuscript, CXCL14 does not compete with CXCL12 to bind with the chemokine receptor CXCR4. We therefore currently do not know the receptor for CXCL14 or the downstream signaling pathways activated. Because of this new data, we propose a change to Task 1b. Instead of assessing competition between CXCL12 and CXCL14, we will instead focus on identifying the CXCL14 receptor. We have already begun this task by identifying CXCL14 binding partners using chemical-modifying linkers and mass spectroscopy. An initial screen identified the desmosomal complex. However, we are concerned about this being a contaminant and are working closely with the University of Michigan Mass Spectroscopy Core Laboratory.

Actual or anticipated problems or delays and actions to resolve them

Difficulties in the CXCL14 shRNA lentivirus have been encountered. Despite another report of the successful mRNA downregulation of CXCL14 using a similar sequence, we have been unable to demonstrate a significant decline in mRNA concentration after transduction of the CXCL14 shRNA lentivirus in the prostate cancer cell line $ARCaP_M$. With the assistance of the University of Michigan Viral Vector Core, we are in the process of generating additional four CXCL14 shRNA lentivirus constructs that will then be tested for successful CXCL14 mRNA knockdown. Once the correct sequence has been identified, we will proceed with the animal model that is detailed in Aim 2a.

Changes that had a significant impact on expenditures
Nothing to report

Significant changes in use or care of vertebrate animals
Nothing to report

6. Products

Publications: The paper entitled “CXCL14 is a Pro-Metastatic Chemokine with CXCR4 Dependent and Independent Actions” was submitted to the Journal *Oncotarget*. A decision of “Accept Pending Major Revisions” was made, and this paper is currently being revised.

7. Participants & Other Collaborating Organizations

Name:	Gregory A. Clines, MD, PhD
Project Role:	PI
Researcher Identifier (e.g. ORCID ID):	N/A
Nearest person month worked:	2.11
Contribution to Project:	Dr. Clines continues to serve as the PI of the projects
Funding Support:	In addition to the DoD grant, Dr. Clines also receives funding support from the Department of Veteran Affairs and the University of Michigan

Name:	Gary Luker, MD
Project Role:	Collaborator
Researcher Identifier (e.g. ORCID ID):	N/A

Nearest person month worked:	0.24
Contribution to Project:	Dr. Luker serves as a collaborator on this project and was instrumental in many of the experimental results as detailed in the attached manuscript.
Funding Support:	In addition to the DoD grant, Dr. Luker also receives funding support from the NIH and the University of Michigan

Name:	Katrina Clines, MS
Project Role:	Lab Manager
Researcher Identifier (e.g. ORCID ID):	N/A
Nearest person month worked:	4.8
Contribution to Project:	Ms. Clines serves as the lab manager is responsible for animal handling and performance/supervising most of the experiments
Funding Support:	In addition to the DoD grant, Ms. Clines also receives salary support from the Department of Veterans Affairs

Name:	Hyun Sik Moon, BS
Project Role:	Laboratory Technician
Researcher Identifier (e.g. ORCID ID):	N/A
Nearest person month worked:	9.0
Contribution to Project:	Mr. Moon has supported and performed many of the experiments in the DoD grant
Funding Support:	In addition to the DoD grant, Mr. Moon also receives salary support from the University of Michigan

Other organizations
Nothing to report

8. Special Reporting Requirements

Nothing to report

9. Appendices

Submitted manuscript: “CXCL14 Is a Pro-Metastatic Chemokine with CXCR4 Dependent and Independent Actions”

CXCL14 Is a Pro-Metastatic Chemokine with CXCR4 Dependent and Independent Actions

Diondra C. Harris[1], Alexander E. Dowell[2], Katrina L. Clines[1], Hyun Sik Moon[1], Charlotte A. Cialek[1], Alexander P. Smith[1], Hui Jiang[3], Colm Morrissey[4], Shi Wei[5], Riley J. Brien[6], Euisik Yoon[6], Yu-Chih Chen[6], Kathryn E. Luker[7], Gary D. Luker[7,8,9], and Gregory A. Clines[1,10]

[1]Department of Internal Medicine, Division of Metabolism, Endocrinology & Diabetes, University of Michigan, Ann Arbor, Michigan

[2]Department of Urology, University of Alabama at Birmingham, Birmingham, Alabama

[3]Department of Biostatistics, University of Michigan, Ann Arbor, Michigan

[4]Department of Urology, University of Washington, Seattle, Washington

[5]Department of Pathology, University of Alabama at Birmingham, Birmingham, Alabama

[6]Department of Electrical Engineering and Computer Science, University of Michigan, Ann Arbor, Michigan

[7]Center for Molecular Imaging, Department of Radiology, University of Michigan, Ann Arbor, Michigan

[8]Department of Microbiology and Immunology, University of Michigan, Ann Arbor, Michigan

[9]Department of Biomedical Engineering, University of Michigan, Ann Arbor, Michigan

[10]Veterans Affairs Medical Center, Ann Arbor, Michigan

Corresponding Author:

Gregory A. Clines, M.D., Ph.D.

Assistant Professor of Internal Medicine

Division of Metabolism, Endocrinology & Diabetes

Department of Internal Medicine

University of Michigan

Endocrinology Section, Ann Arbor VA Medical Center

2215 Fuller Road, Research 151

Ann Arbor, Michigan 48105-2399

Office: (734) 845-3443

Email: clines@umich.edu

Keywords: Prostate cancer; bone metastasis; CXCL14; CXCL12; CXCR4

Number of Figures: 7

Number of Tables: 0

ABSTRACT

The chemokine CXCL14 has complex effects on tumorigenesis but its role in promoting bone metastasis is unknown. The expression of CXCL14 in prostate cancer bone metastasis was investigated using a human prostate cancer tissue microarray. CXCL14 expression was significantly higher in bone metastases compared to normal prostate, benign prostatic hypertrophy, primary prostate cancer, and metastases to lymph nodes and soft tissues. Investigations were performed to understand the biology of CXCL14 as a pro-metastatic prostate cancer chemokine. CXCL14 stimulated *in vitro* migration and invasion of the human prostate cancer cell line $ARCaP_M$, and promoted expression of epithelial-to-mesenchymal transition-associated genes in $ARCaP_M$ and PC-3 prostate cancer cells. Moreover, CXCL14 activated MAPK and PI3K/AKT signaling pathway proteins. CXCL14 signaling activation was not due to direct interaction with the chemokine receptor CXCR4, addressing controversy as to the identity of the CXCL14 chemokine receptor. CXCL14 did not activate CXCR4 signaling in a luminescent complementation reporter assay that detects CXCR4 recruitment of β-arrestin 2. Furthermore, an interaction of CXCL14 with CXCR4 or CXCR7 was not detected using a sensitive luminescent complementation assay. Despite the lack of a direct CXCL14/CXCR4 interaction, CXCL14-activated migration was dependent on CXCR4 as demonstrated using a novel microfluidic cell migration assay. Together, these data suggest that CXCL14 interacts with an unidentified chemokine receptor that may have cooperative actions with CXCR4. This investigation identified CXCL14 as a novel

prostate cancer pro-metastatic chemokine and may represent an appealing target for the treatment of prostate cancer bone metastasis.

INTRODUCTION

Chemokines and their receptors were originally identified as mediators of inflammatory disease processes but were later discovered to function as crucial links between tumor cells and stromal cells, strongly promoting proliferation, migration and invasion through multiple signaling pathways [1, 2]. The C-X-C chemokine receptor type 4 (CXCR4) is overexpressed in many different cancer types including cancers of the prostate, breast, lung, and pancreas [2, 3]. CXCL12 (stromal cell-derived factor-1/SDF-1), a CXCR4 ligand, is a chemoattractant that facilitates the migration of CXCR4-expressing primary tumor cells towards metastatic sites [4]. Prostate cancers (PCa), in particular, exploit the CXCL12/CXCR4 axis to “home” to bone [5, 6]. PCa cells migrate across bone marrow endothelial cell monolayers in response to CXCL12 [7]. Additionally, the invasion of PC-3, LNCaP and C4-2B human PCa cell lines into a reconstituted extracellular matrix was inhibited when CXCR4 expression was decreased [8]. The work by Xing, *et al* confirmed and extended these findings—stable knockdown of CXCR4 blocked CXCL12-dependent PCa cell adhesion to osteosarcoma and endothelial cells, inhibited *in vitro* invasion, and reduced PCa skeletal growth after intratibial inoculation in immunodeficient mice [9].

Although CXCL12 has been a focus in numerous published reports, the related chemokine CXCL14 (earlier designated as BRAK) has been implicated in metastasis as well. CXCL14 is a 77-amino acid secreted protein and member of the C-X-C chemokine family [10]. This chemokine displays activity in immature dendritic cells, monocytes, macrophages and NK cells [11]. CXCL12 and CXCL14 are primordial chemokines and

possess close evolutionary sequence conservation with each other as well as orthologous conservation among distantly related species [12]. It has been suggested that CXCL12 and CXCL14 have cooperative actions because of non-overlapping expression in adjacent tissues present during chick and mouse eye development [13].

CXCL14 expression in cancers, compared to normal tissues, had been reported to be both increased and decreased depending cell type. CXCL14 was downregulated in breast cancer, hepatocellular carcinoma, gastric cancer, colon cancer, mouse acute myeloid leukemia, and neuroendocrine tumors [14-21]. However, CXCL14 expression was increased in gliomas, colon cancer, and BRAF-mutant papillary thyroid [22-24]. CXCL12 and CXCL14 expression within tumor-associated mesenchymal cells was significantly greater in breast cancer metastases to bone compared to metastases to lung, liver, or brain [25, 26]. CXCL14 had been implicated in both promoting and inhibiting cancer cell motility, proliferation, invasion, and metastasis in several reported models [27-30]. CXCL14 has pleiotropic effects that are dependent on context and cancer type.

CXCL14 may have tumor-promoting actions in PCa as well. A genetic approach was utilized to identify PCa susceptibility genes in a genetic cross utilizing the TRAMP mouse model of PCa. CXCL14 was one of five genes identified that correlated with primary tumor burden. Furthermore, a single nucleotide polymorphism within the human CXCL14 gene was found associated with PCa tumor progression [31].

Until now, an association of CXCL14 with PCa bone metastasis was unknown. The study reported here was designed to investigate the expression and clinical significance of CXCL14 in PCa bone metastasis. CXCL14 expression was increased in PCa cells

metastatic to bone but unchanged in other metastatic sites compared to normal prostatic tissue in a tissue microarray. *In vitro* assays showed that CXCL14 activated PCa signaling pathways, chemotaxis, and may be important for EMT. Luminescent biocomplementation assays revealed the existence of a CXCL14 homodimer and that CXCL14 does not possess a strong affinity for CXCR4 but at the same time is dependent on CXCR4 for chemotaxis. CXCL14 represents a newly recognized factor in the pathogenesis of PCa bone metastasis.

RESULTS

Increased PCa CXCL14 Expression in Bone Metastasis

A cohort of patient samples from 28 histologically normal prostates, 30 benign prostatic hypertrophies (BPH), 52 primary prostate cancers (Gleason grade 3-5), 34 lymph node metastases, 27 soft tissue metastases and 113 bone metastases tissue samples were used to construct a tissue microarray (TMA). This TMA set was analyzed for CXCL14 protein expression. CXCL14 quantification was determined by an H-score that encompassed both % positive cell number and intensity of stain. No significant difference in H-score was detected in normal prostate compared to BPH, primary PCa, lymph node metastasis and soft tissue metastasis. A significant increase in CXCL14 expression was detected in bone metastasis compared to all other groups (Figure 1A). Immunohistochemical CXCL14 staining was almost exclusively restricted to the cytoplasm (Figure 1B). A secondary analysis was performed to assess correlation of

CXCL14 H-score with primary PCa Gleason grade. No association was detected (Figure 1C). These data support an increase in CXCL14 expression after arrival of PCa to bone.

CXCL14 Stimulates Migration and Invasion of PCa

In vitro scratch migration and transwell invasion assays were performed on human PCa cell lines ($ARCaP_M$ and PC-3) to assess the effects of CXCL14. In the scratch assay, $ARCaP_M$, but not PC-3, cells robustly responded to CXCL14 after 24 hours of treatment (Figure 2A).

Transwell invasion assays were then performed. PCa cells were plated on a cell matrix above a porous membrane. The extent to which cells migrated through these barriers towards a CXCL14 gradient on the opposite side of the membrane was examined. After 72 hours, a minimal invasive response was found with PC-3 PCa cells, as compared to no treatment group. However, $ARCaP_M$ cell invasion was significantly increased with CXCL14 treatment (Figure 2B).

CXCL14 Regulates the Expression of SLUG, SNAIL, and TWIST

Activation of epithelial-to-mesenchymal transition (EMT) has been implicated as a contributor to cancer invasion and metastasis [32]. The effects of CXCL14 to regulate genes associated with a metastasis phenotype were investigated to further establish that CXCL14 promotes PCa metastatic behavior. Real-time RT PCR was performed on the $ARCaP_M$ and PC-3 PCa cell lines. A dose response of *SLUG*, *SNAIL* and *TWIST*

mRNA expression to increasing CXCL14 treatment concentrations was detected in the $ARCaP_M$ PCa cells (Figure 3A).

Interestingly, treatment of PC-3 cells with 10 ng/ml CXCL14 down-regulated transcripts for genes associated with EMT (Figure 3B). However, higher concentrations of CXCL14 restored *TWIST* and *SNAIL* to baseline. *SLUG* expression in PC-3 cells was increased with CXCL14 100 and 200 ng/ml treatments. These data suggest a mechanism of increased migration and invasion may be associated with expression of EMT genes.

Regulation of Kinase Signaling by CXCL14

CXCL12 activates MAPK and PI3K signaling pathways in a number of different cell types [8, 33-35]. MAPK and PI3K signaling pathways have been linked to uncontrolled growth and resistance to apoptosis during tumor progression [36]. The extent to which CXCL14 activated similar pathways was examined. PC-3 and $ARCaP_M$ cells were treated with CXCL14 250 ng/ml for 10-120 minutes. Western blot analysis assessed ERK-1/ERK-2, AKT, SAPK/JNK, NF-κB, and p-38 signaling pathway activation upon CXCL14 treatment.

Rapid phosphorylation of AKT, ERK, SAP/JNK, NF-κB and p-38 proteins was observed within 10-30 minutes of CXCL14 treatment. $ARCaP_M$ cells responded with a marked increase in ERK, p38, and SAPK/JNK phosphorylation at 10 and 30 minutes that returned to baseline after 1-2 hours (Figure 4A). Persistent NF-κB phosphorylation remained at two hours. PC-3 cells demonstrated AKT and NF-κB phosphorylation after 30 minutes of stimulation (Figure 4B) but no detectable phosphorylation of SAPK/JNK

or p-38 (data not shown). Although an increase in activation of signaling molecules was detected in both cell lines, only ARCaP$_M$ cells demonstrated a significantly robust increase in multiple phosphorylated signaling proteins that corroborates earlier reported cellular effects of CXCL14.

Lack of CXCL14-Dependent β-Arrestin 2 Recruitment to CXCR4

CXCL14 stimulated migration, invasion, EMT associated genes, and MAPK signaling mainly in ARCaP$_M$ cells, yet the mechanism of signal transduction remained unclear. The structurally similar CXCL12 binds CXCR4 and recruits the cytosolic adaptor protein β-arrestin 2 that functions as a scaffold protein linking G protein-coupled receptors (GPCRs) to intracellular signal transduction pathways [37].

The availability of tools to adequately study CXCL14 and CXCR4 signaling in prostate cancer was lacking. We therefore utilized research resources currently available to better understand mechanisms of CXCL14 cellular action. To assess CXCL14-dependent recruitment of β-arrestin 2, the validated MDA-MB-231 click beetle green luciferase complementation reporter system was used to examine mechanisms of CXCL14 signaling [38-40]. In this system, the MDA-MB-231 cell line was transduced with fusion proteins CXCR4-CBRN and β-arrestin 2-CBC. Activation of CXCR4 recruits β-arrestin 2 and joins the incomplete luciferase products to generate an active luciferase molecule.

As a control for CXCL14 biologic activity, the transduced MDA-MB-231 cells were treated with CXCL14. A marked increase in AKT phosphorylation at 10 minutes was observed (Figure 5A). Cells that stably expressed the complementation reporters were

treated with CXCL14 and CXCL12 individually and combined at concentrations of 60 ng/ml (Figure 5B) and 250 ng/ml (Figure 5C). Cells were serially imaged for up to 120 minutes. Luciferase activity increased rapidly, in a dose-dependent manner, with CXCL12 but not with CXCL14 treatment. Moreover, the addition of CXCL14 to CXCL12 did not lessen the ability of CXCL12 to recruit β-arrestin 2 to CXCR4.

Upon chemokine ligand binding to CXCR4, the CXCR4/β-arrestin 2 complex is internalized resulting in less cell surface receptor available for ligand binding. The availability of surface CXCR4 following CXCL12 treatment was determined using the MDA-MB-231 CXCR4-CBRN/β-arrestin 2-CBC reporter system. The reporter cells were pretreated with either CXCL12 or CXCL14 in increasing concentrations for one hour followed by a subsequent CXCL12 200 ng/ml treatment at which time luminescence was monitored (Figure 5D). The peak signal was plotted for each chemokine concentration. Pretreatment with increasing concentration of CXCL14 did not alter CXCR4-CBRN/β-arrestin 2-CBC association. However, pretreatment with CXCL12 showed concentration-dependent decreases in further luminescence produced by adding additional CXCL12 that is consistent with receptor internalization and desensitization of signaling. These data suggested that CXCL14 does not promote CXCR4 receptor internalization and that CXCR4 is not a CXCL14 receptor.

CXCL14 Ligand Dimerization and Chemokine Receptor Association

CXCL12 exists in both monomeric and dimeric forms at physiologic concentration [41, 42]. Each of these CXCL12 species activates CXCR4 but differs in the downstream signaling pathways activated [42]. The extent to which CXCL14 exists as a homodimer

or heterodimer with other chemokines such as CXCL12 was investigated. A similar complementation strategy as reported above, using the NanoLuc luminescent complementation reporter system, was utilized to examine these interactions. CXCL14, CXCL12, and an irrelevant control protein were cloned in-frame, each receiving adjacent NanoLuc large fragment (LgBit) or the NanoLuc small fragment (SmBit). The combination of the LgBit and SmBit results in a complete and active luminescent protein. HEK-293T cells were co-transfected with various combinations of CXCL14, CXCL12, and the irrelevant protein, followed by luminescent imaging of intact cells and of the conditioned media. This represented a strategy to detect homo- and heterodimer species located within the cellular fraction and in the media. Increased luminescence above what was detected in the chemokine/irrelevant protein combinations was evidence for an interaction.

In the cellular fraction, both CXCL12 and CXCL14 homodimer luminescence was significantly greater than the chemokine/irrelevant heterodimer control indicating the existence of CXCL12 and CXCL14 homodimers (Figure 6A). A CXCL12/CXCL14 heterodimer was also detected, albeit at levels lower than either homodimer. Luminescence was also detected in the conditioned media of cells but at a lower concentration compared to the cell-associated fraction. In the secreted fraction, the luminescence level trended higher for both the CXCL12 and CXCL14 homodimer group but the level was not statistically different compared to the chemokine/irrelevant heterodimer controls. Similarly, the existence of a CXCL12/CXCL14 heterodimer was not detected in the secreted fraction. These data indicate that CXCL12 and CXCL14 homodimers, and a CXCL12/CXCL14 heterodimer exist at higher concentrations within

secretory vesicles, but that once secreted from the cell the chemokines revert to monomers.

CXCR4 and CXCR7 (also known as ACKR3) are receptors for CXCL12 [43, 44]. Using the NanoLuc complementation assay, the physical association of CXCL14 with CXCR4 and CXCR7 was investigated. As expected and previously reported, CXCL12/CXCR4 and CXCL12/CXCR7 interactions were detected (Figure 6A). However, an interaction between CXCL14 and the two tested chemokine receptors was not detected.

Dependence of CXCR4 on CXCL14-Mediated Cellular Migration

A novel microfluidic migration platform has been developed to measure the cellular response to a chemotactic agent [45]. This platform consists of 300 microfluidic channel devices. Single cells enter the channels and responsive cells migrate toward the end of the channel containing the chemoattractant. At treatment completion, the final location of individual cells is determined by microscopic imaging.

To assess the chemotactic effects of CXCL14, the microfluidic cell migration assay was employed in conjunction with a panel of SUM159 breast cancer cells. Wild-type (WT) SUM159 cells express physiologic levels of CXCR4; the CXCR4 gene was deleted with Crispr/Cas9 gene editing (KO). KO cells with re-expressed CXCR4 (Add-Back) were also generated. The three cell populations were loaded in quadruplicate devices. No treatment or CXCL14 10 nM (94 ng/ml) was used as the chemoattractant and the microfluidic devices were imaged 24 hours later. Due to the complexity of these experiments, the no treatment group and CXCL14 treatment group assays were

performed on separate days. In the absence of CXCL14, the migratory distribution of WT, KO and Add-Back cells was unchanged (Figure 7). However, in the presence of CXCL14, CXCR4 KO resulted in fewer cells migrating compared to WT; the add-back of CXCR4 restored migratory potential. These data supported that CXCL14 is, at least partially, dependent on CXCR4 for cell migration.

DISCUSSION

CXCL14 is associated with cancer metastasis in *in vitro*, pre-clinical, and clinical studies, but a unifying mechanism for CXCL14 as a regulator of PCa bone metastasis had not been clearly defined [23, 27-29, 31, 46-48]. This report is the first to identify CXCL14 as a promoter of PCa bone metastatic. In a PCa tissue microarray, CXCL14 expression was significantly higher in PCa cells that had metastasized to bone compared to normal prostate and extra-skeletal PCa metastasis. This increase in expression could not be explained by the Gleason grade of the primary tumor. Based on the data presented here, either the bone microenvironment is regulating PCa CXCL14 expression or rare bone metastatic PCa stem cells within the primary tumor are overexpressing CXCL14. The mechanism of increased PCa expression in bone is an area of future study.

CXCL14 may, in fact, reinforce the well-known biological effects of CXCL12, such as invasiveness and genes that promote metastasis, and exhibit at least a partial overlap in function during PCa bone metastasis. Normally, CXCL12 is secreted by bone marrow stromal cells in perivascular spaces [49] and directs the migration of CXCR4-expressing hematopoietic precursors to the bone marrow microenvironment [1, 50-53]. Prostate

cancers exploit and hijack this signaling pathway to direct CXCR4-expressing PCa cells to the skeleton. In previous studies, PCa CXCR4 activation increased EMT, via expression of *TWIST*, *SNAIL* and *SLUG* [54-57]. CXCL14 exhibited a similar response in the PCa cell line ARCaP$_M$, but not PC-3 cells, with increased invasiveness and pro-metastatic genes. The differential effects of CXCL14 reported here are aligned with other studies reporting CXCL14 pleiotropic effects that are dependent on context and cell type. One notable example is a study that examined two non-small cell lung cancer cell lines, in which a high-affinity CXCL14 unknown receptor was present in both, but CXCL14 treatment elicited unrelated effects between the two cell lines [28].

Initiation of signaling pathways by CXCL14 is likely occurring through chemokine receptor activation resulting in activation of kinase signaling pathways that include ERK, AKT, SAPK/JNK, and NF-κB. The elusive CXCL14 receptor had been reported to be CXCR4. Tanegashima, *et al* reported that a high affinity binding site or sites exists on the human monocytic cell line THP-1 and that knockdown of CXCR4 in this cell line reduced CXCL14 high-affinity binding [58]. Moreover, CXCL14 was reported to co-immunoprecipitate with CXCR4. The conclusions of this report were disputed by Otte *et al* that asserted that CXCL14 is not a CXCR4 ligand and that CXCL14 did not modulate CXCL12-mediated CXCR4 receptor phosphorylation, GPCR Ca^{2+} signaling, ERK phosphorylation, or CXCL12-mediated CXCR4 receptor internalization [59]. In a more recent report, Collins *et al* propose a mechanism in which CXCL14 binds to a CXCR4 homodimer that displaces CXCL12 from the adjacent CXCR4 dimer and effectively downregulates CXCL12 activation of CXCR4 [60]. In the study reported here, CXCL14 did not interact with CXCR4 in a luminescent complementation assay, and CXCL14 was

unable to recruit β-arrestin 2 to CXCR4. However, in the microfluidic migration assay, CXCL14 was clearly dependent on CXCR4 for the migratory response.

These apparent inconsistencies as to whether CXCL14 is a true CXCR4 ligand or not can be reconciled with a model in which the putative CXCL14 chemokine receptor heterodimerizes with CXCR4. Although CXCL14 may not directly bind CXCR4, its actions may be dependent on CXCR4. Precedence for CXCR4 heterodimers with CXCR7, CCR2, CCR5, the cannabinoid receptor 2 (CB2), and the opioid receptor delta have been reported [61-65]. The previously published reports of Tanegashima, *et al*, Otte, *et al*, and Collins *et al* would be consistent with this hypothesis. Another consideration is that CXCL14 forms a heterodimer with a chemokine other than CXCL12, and that crosstalk within these multimers allows for regulation of chemokine receptors in response to stimuli. Because CXCL14 demonstrated no significant direct interaction with CXCR4, the effects on CXCR4 signaling pathway may occur through multimers in complex with the CXCL14 receptor or receptors. Future work is needed to identify the true CXCL14 receptor.

Bone metastasis is a painful consequence of PCa in men with advanced disease. The chemokine CXCL14 has been identified as a promoter of PCa bone metastasis. CXCL14 may in fact reinforce CXCL12-mediated events only after arrival of PCa to bone, promoting residency of tumor cells in bone. The identification of the CXCL14 receptor, combined with understanding of the shared and dissimilar actions with CXCL12, is a new research avenue that may lead to a novel therapeutic target in men with metastatic PCa.

MATERIALS AND METHODS

Human PCa Tissue Microarray

Normal human prostate, and primary and metastatic PCa tissues were obtained through the University of Washington Medical Center Prostate Cancer Donor Rapid Autopsy Program. Samples were obtained from patients who had died of metastatic castrate-resistant prostate cancer (CRPC). Rapid autopsy was performed within 2-10 hours of death, under the support of the Prostate Cancer Donor Program at the University of Washington [66]. The Institutional Review Board of the University of Washington Medical Center approved all procedures involving human subjects, and all subjects signed written informed consent. Tissue samples were collected from bone, metastatic lymph nodes, liver, and lung in a systematic and consistent fashion in every case. A human tissue microarray was constructed from 44 patients with 185 metastatic sites and consisted of the following: 28 histologically normal prostates, 30 benign prostatic hypertrophies (BPH), 52 primary PCa (Gleason grade 3-5), 34 lymph node metastases, 27 soft tissue metastases and 113 bone metastases tissue samples. Each metastatic site was represented by two cores. Five μm tissue sections were probed with a mouse anti-human CXCL14 antibody (MAB866, 5μg/ml; R&D Systems, Minneapolis, MN) and visualized with 3,3'-dioaminobenzidine (DAB). Staining intensity of PCa cells (0-absent; 1+ faint; 2+ moderate; 3+ intense) and percentage of cells at the staining intensity were determined, and the H-score was calculated [H-score = 1X (% 1+ cells) + 2X (% 2+ cells) + 3X (% 3+ cells)].

Cell Culture

The $ARCaP_M$ cell line (Novicure Biotechnology, Birmingham, AL) was derived by single cell cloning of the parental ARCaP cells [67]. The $ARCaP_M$ cell line was maintained in MCaP growth medium (Novicure Biotechnology) supplemented with 5% fetal bovine serum (FBS). The PC-3 human PCa cell line was purchased from the American Type Culture Collection (ATCC, Manassas, VA). PC-3 cells were maintained in F-12K medium supplemented with 10% FBS. Human PCa cells were maintained in RPMI medium supplemented with 10% FBS. MDA-MB-231 cells were purchased from ATCC and maintained in DMEM medium supplemented with 10% FBS. The SUM159 breast cancer cell line was obtained from Dr. Stephen Ethier (Medical University of South Carolina) and maintained in Ham's F-12 medium with 10% FBS, 5 μg/ml insulin, and 1 μg/ml hydrocortisone. All cell lines were grown in a humidified incubator with 5% CO_2 at 37°C and supplemented with 100 I.U./ml penicillin and 100 μg/ml streptomycin.

Scratch Migration Assay

Twelve-well plates were coated with Matrigel® (Corning Inc., Corning, NY). $ARCaP_M$ and PC-3 cells were plated and grown to confluency. Thereafter, these cells were treated with 0.5% FBS with or without CXCL14 250 ng/ml overnight. The following day, the bottom of the well was scratched with a pipette tip. After several washes with serum-free medium, cells were incubated with 0.5% serum-containing medium with or without CXCL14 250 ng/ml corresponding to their corresponding pre-treatment. Images of cell migration into the scratch were captured at 0, 6, and 24 hour intervals. Analyses of cells that migrated into the scratch area were performed using the ImageJ software package.

Transwell Migration Assay

Transwell® inserts with 8-μm pores (Corning Inc., Corning, NY) were coated with Matrigel® (Corning). Approximately 200,000 $ARCaP_M$ or PC-3 cells were added to the inserts in media containing 0.5% FBS and allowed to attach overnight. The following day, media containing 0.5% FBS, 10% FBS or 0.5% FBS/CXCL14 250ng/ml were added to the bottom of respective wells, and the plates were incubated in a humidified incubator with 5% CO_2 at 37°C. After 72 hours, Transwell inserts and wells were washed with PBS, calcein AM 8 μM (ThermoFisher Scientific) was placed at the bottom of each well, and plates were incubated for 10 minutes. Next, 10 μl of 10X trypsin was added to each well, and incubated for 10 additional minutes. Transwell plates were gently agitated on the shaker for 1 minute. Contents of each well were plated in a 96-well black-walled plate, and fluorescence was measured using a plate reader (495 (ex)/515 (em) nm).

Real-Time RT PCR

Confluent $ARCaP_M$ and PC-3 PCa cells were treated with various concentrations of CXCL14 (0, 10, 100, and 200 ng/ml) in media supplemented with 0.5% FBS for 24 hours in a humidified incubator with 5% CO_2 at 37°C. Cells were washed in ice-cold PBS and RNA was extracted (Zymo Direct-zol kit, Irvine, CA). A DNase digestion step was included during RNA purification. Real-time RT PCR was performed using the iQ SYBR Green Supermix kit (Bio-Rad, Hercules, CA). Changes in mRNA concentration were determined using the $2^{-[\Delta][\Delta]Ct}$ method and *RPL32* was used as the internal control.

Amplification was performed using primers specific to human *SNAIL*, *SLUG*, and *TWIST*. (*SNAIL* forward: gaccccaatcggaagcctaa; *SNAIL* reverse: agggctgctggaaggtaaac; *SLUG* forward: gactaccgctgctccattcc; *SLUG* reverse: actcactcgccccaaagatg; *TWIST* forward: gtccgcagtcttacgaggag; *TWIST* reverse: atcttgctcagcttgtccga; *RPL32* forward: cagggtgcggagaaggttcaaggg; *RPL32* reverse: cttagaggacacgttgtgagcaat).

Western Blot Analyses

ARCaP$_M$ and PC-3, at 80% confluence, were serum-starved in medium supplemented with 0.1% bovine serum albumin (Probumin, Celliance) for 8 hours. Serum-starved cells were treated with 250 ng/ml of CXCL14 for 0, 10, 30, 60, and 120 minutes. Thereafter, cells were washed in ice-cold PBS. Cells were lysed in mammalian extraction protein reagent (M-PER) lysis buffer (ThermoFisher Scientific) that contained protease and phosphatase inhibitors. Cell lysates were subjected to SDS-PAGE and transferred onto PVDF membranes. Membranes were blocked using 5% milk. Antibodies specific for phospho-AKT (Ser473), AKT, Phospho-p38 MAPK (Thr180/Tyr182), Phospho-p44/42 MAPK (ERK1/2) (Thr202/Tyr204), Phospho-SAPK/JNK (Thr183/Tyr185) and GAPDH (Cell Signaling, Danvers, MA) were diluted in TBS buffer at a 1:1000 ratio. Membranes were incubated with antibodies overnight at 4°C, followed by a horseradish peroxidase-conjugated mouse anti-rabbit secondary antibody (Cell Signaling) and western blot detection reagent. Bands were visualized using a luminescent imager (ChemiDoc Bio-Rad, Hercules, CA). Experiments were performed at least three times.

Luciferase Complementation Reporter Assay for CXCR4 Activation

Generation of MDA-MB-231 human breast cancer cells stably expressing CXCR4-CBRN and β-arrestin 2-CBC was previously described [38]. Cells were plated at 20,000 cells per well in 96-well black-walled plates. Cells were grown in a humidified incubator with 5% CO_2 at 37°C for two days. After a two-day incubation, medium was replaced with 50 µl phenol red free DMEM (Life Technologies) with 0.2% media grade bovine serum albumin (Probumin, Celliance, Billerica, Ma,) 30 minutes before imaging. Next, 7 µL of a 15 mg/ml luciferin stock was added to cells and incubated for 5 minutes before the addition of chemokine treatments. Immediately before imaging, 14 µL phenol red-free DMEM containing 0.2% media grade bovine serum albumin was added with increasing concentrations of CXCL12 (R&D Systems, Minneapolis, MN) and/or CXCL14 (Cat# ab174986, Abcam, Cambridge, MA). Luminescent imaging with an IVIS Lumina (Perkin-Elmer, Waltham, MA) was performed at 37°C with 2 minute exposures at large binning at the indicated times. To determine relative induction of bioluminescence, bioluminescence was normalized in wells treated with chemokines to cells incubated with vehicle control at each time point (n=4 per condition).

NanoLuc Luminescence Assays

Plasmids were constructed expressing proteins fusions to NanoLuc luciferase or NanoBit fragments LgBit or SmBit for protein fragment complementation (Promega, Madison, WI). Details of the plasmid constructions are in Supplementary Materials.

HEK-293T cells (140,000 cells/well in 12-well plates) were cultured in DMEM with 10% FBS with 1% Pen/Strep/Glutamine. Cells were transfected with 250 ng of each plasmid alone or in pairs using calcium phosphate transfection. Transfected cells were transferred 24 hours later to 96-well black-walled cell culture plates with 10,000 cells/well in 100 µl media. Luminescence assays of cells and media were performed 48 hours after transfection, as indicated. Luminescence was measured with an IVIS Lumina (Perkin-Elmer) in cells or cell supernatants using a final concentration of 1 µg/ml furimazine (Nano-Glo Live Cell Assay, Promega) diluted into media or PBS.

Crispr/Cas9 deletion of CXCR4 from SUM159 cells

CXCR4 was knocked out in SUM-159 cells by CRISPR/Cas9 gene editing using the pGuide-it CRISPR/Cas9 system from Takara Bio USA (Mountain View, CA), expressing Cas9, a fluorescent protein tdTomato, and a sgRNA 5' GTACAGGCTGCACCTGTCAG 3’ targeted near the 5’ end of the second exon of human CXCR4. Cells (100,000) were transfected in 6-well plates using Fugene HD from Promega (Madison, WI), sorted by flow cytometry for expression of tdTomato into 96-well plates and cultured as clonal sublines. To facilitate sequencing of all CXCR4 alleles in a subline, the region of the genome targeted by the sgRNA was amplified by PCR of cell lysates with flanking primers 5’ ccttagcccactacttcagaatttcctgaagaaagc 3’ and 5’gcataggaagttcccaaagtaccagtttgccacgg 3’ and subcloned for DNA sequencing of individual alleles. Two SUM-159 CXCR4 knockout sublines were verified by sequencing to have deletions in all alleles which resulted in complete absence of in-frame

transcript. Both clones exhibited similar phenotypes in tests for CXCR4 function (data not shown), so a single clone was chosen for this study.

Microfluidic Cell Migration Assay

Cell migration assays were performed using a previously published microfluidic migration platform [45, 68]. To achieve higher throughput, the design was modified to have 300 migration channels per device, and the migration channel was designed to be 5 μm in height, 30 μm in width, and 1 mm in length. Before cell loading, PBS was used to prime the device for one hour, and the cell culture medium flowed through the channel for one hour for better cell adhesion and viability. The cells were trypsinized, centrifuged, and then re-suspended to a concentration of 4X 10^5 cells/ml for loading into the device. After cell loading, the cell suspension in the left inlet was replaced with serum-free cell culture media, and 10 nM (94 ng/ml) CXCL14 was applied to the other inlet to induce chemotactic migration. The microfluidic chip was then put into an incubator, and migration distance was measured based on the final cell position after 24 hours of incubation without medium replenishment. The images were analyzed by custom MATLAB code automatically [69]. Cells were identified based on their fluorescence, and debris was ignored by their small size. A comparison between MDA-MB-231 (known to be motile) and T47D (known to be non-motile) breast cancer cells served as the validation of the platform (data not shown). For all conditions in this work, 4 replicates (total of 1,200 channels) were performed.

Statistics

In experiments with two experimental groups, a standard t-test was performed. In three or more experimental groups, a one-way ANOVA was performed followed by Tukey's multiple comparison test. Microfluidic migration assay results were analyzed using two-way ANOVA with Tukey's multiple comparison test. A p-value ≤ 0.05 was considered significant. Data were graphed as mean values, using standard deviation (SD) or standard error of the mean (SEM).

ABBREVIATIONS

CXCL14: Chemokine (C-X-C motif) ligand 14

CXCL12: Chemokine (C-X-C motif) ligand 12

CXCR4: C-X-C chemokine receptor type 4

PCa: Prostate cancer

BPH: Benign prostatic hypertrophy

TMA: Tissue microarray

EMT: Epithelial-to-mesenchymal transition

LgBit: NanoLuc large fragment

SmBit: NanoLuc small fragment

AUTHOR CONTRIBUTIONS

DCH, AED, CAC, KEL, GDL and GAC were involved in the study design; DCH, AED, KLC, HSM, CAC, APS, SW, RJB, EY, Y-CC, KEL conducted the study; DCH, AED, HSM, CAC, SW, Y-CC, KEL collected the data; DCH, AED, CAC, HJ, Y-CC, KEL analyzed the data, DCH, AED, CAC, HJ, KEL, GDL and GAC interpreted the data; DCC and GAC drafted the manuscript; all authors provided edits and approved in the final version of the manuscript.

CONFLICTS OF INTEREST

The authors disclose no potential conflicts of interest.

ACKNOWLEDGEMENTS AND FUNDING

This work was supported by the Department of Defense Prostate Cancer Research Program to G.C. (PC140357); NIH grants CA170198, CA196018, and CA195655 to G.D.L; NIH PO1 CA163227; and the PNW Prostate Cancer SPORE NIH P50 CA097186. We thank the patients and their families, Robert Vessella, Paul Lange, Celestia Higano, Bruce Montgomery, Evan Yu, Peter Nelson, Martine Roudier, and Lawrence True for their contributions to the University of Washington Medical Center Prostate Cancer Donor Rapid Autopsy Program.

REFERENCES

1. Guo F, Wang Y, Liu J, Mok SC, Xue F, Zhang W. CXCL12/CXCR4: a symbiotic bridge linking cancer cells and their stromal neighbors in oncogenic communication networks. Oncogene. 2016; 35: 816-26. doi: 10.1038/onc.2015.139.
2. Chatterjee S, Behnam Azad B, Nimmagadda S. The intricate role of CXCR4 in cancer. Adv Cancer Res. 2014; 124: 31-82. doi: 10.1016/B978-0-12-411638-2.00002-1.
3. Muller A, Homey B, Soto H, Ge N, Catron D, Buchanan ME, McClanahan T, Murphy E, Yuan W, Wagner SN, Barrera JL, Mohar A, Verastegui E, et al. Involvement of chemokine receptors in breast cancer metastasis. Nature. 2001; 410: 50-6. doi: 10.1038/35065016.
4. Mukherjee D, Zhao J. The Role of chemokine receptor CXCR4 in breast cancer metastasis. Am J Cancer Res. 2013; 3: 46-57. doi:
5. Sun YX, Schneider A, Jung Y, Wang J, Dai J, Wang J, Cook K, Osman NI, Koh-Paige AJ, Shim H, Pienta KJ, Keller ET, McCauley LK, et al. Skeletal localization and neutralization of the SDF-1(CXCL12)/CXCR4 axis blocks prostate cancer metastasis and growth in osseous sites in vivo. Journal of Bone & Mineral Research. 2005; 20: 318-29. doi:
6. Gladson CL, Welch DR. New insights into the role of CXCR4 in prostate cancer metastasis. Cancer Biol Ther. 2008; 7: 1849-51. doi:

7. Taichman RS, Cooper C, Keller ET, Pienta KJ, Taichman NS, McCauley LK. Use of the stromal cell-derived factor-1/CXCR4 pathway in prostate cancer metastasis to bone. Cancer Res. 2002; 62: 1832-7. doi:
8. Wang J, Wang J, Sun Y, Song W, Nor JE, Wang CY, Taichman RS. Diverse signaling pathways through the SDF-1/CXCR4 chemokine axis in prostate cancer cell lines leads to altered patterns of cytokine secretion and angiogenesis. Cell Signal. 2005; 17: 1578-92. doi: 10.1016/j.cellsig.2005.03.022.
9. Xing Y, Liu M, Du Y, Qu F, Li Y, Zhang Q, Xiao Y, Zhao J, Zeng F, Xiao C. Tumor cell-specific blockade of CXCR4/SDF-1 interactions in prostate cancer cells by hTERT promoter induced CXCR4 knockdown: A possible metastasis preventing and minimizing approach. Cancer Biol Ther. 2008; 7: 1839-48. doi:
10. Hara T, Tanegashima K. Pleiotropic functions of the CXC-type chemokine CXCL14 in mammals. J Biochem. 2012. doi: 10.1093/jb/mvs030.
11. Shurin GV, Ferris RL, Tourkova IL, Perez L, Lokshin A, Balkir L, Collins B, Chatta GS, Shurin MR. Loss of new chemokine CXCL14 in tumor tissue is associated with low infiltration by dendritic cells (DC), while restoration of human CXCL14 expression in tumor cells causes attraction of DC both in vitro and in vivo. J Immunol. 2005; 174: 5490-8. doi:
12. Huising MO, van der Meulen T, Flik G, Verburg-van Kemenade BM. Three novel carp CXC chemokines are expressed early in ontogeny and at nonimmune sites. Eur J Biochem. 2004; 271: 4094-106. doi: 10.1111/j.1432-1033.2004.04347.x.

13. Ojeda AF, Munjaal RP, Lwigale PY. Expression of CXCL12 and CXCL14 during eye development in chick and mouse. Gene Expr Patterns. 2013; 13: 303-10. doi: 10.1016/j.gep.2013.05.006.
14. Bu D, Lewis CM, Sarode V, Chen M, Ma X, Lazorwitz AM, Rao R, Leitch M, Moldrem A, Andrews V, Gazdar A, Euhus D. Identification of breast cancer DNA methylation markers optimized for fine-needle aspiration samples. Cancer Epidemiol Biomarkers Prev. 2013; 22: 2212-21. doi: 10.1158/1055-9965.EPI-13-0208.
15. Gu XL, Ou ZL, Lin FJ, Yang XL, Luo JM, Shen ZZ, Shao ZM. Expression of CXCL14 and its anticancer role in breast cancer. Breast Cancer Res Treat. 2012; 135: 725-35. doi: 10.1007/s10549-012-2206-2.
16. Wang W, Huang P, Zhang L, Wei J, Xie Q, Sun Q, Zhou X, Xie H, Zhou L, Zheng S. Antitumor efficacy of C-X-C motif chemokine ligand 14 in hepatocellular carcinoma in vitro and in vivo. Cancer Sci. 2013; 104: 1523-31. doi: 10.1111/cas.12279.
17. Hu C, Lin F, Zhu G, Xue X, Ding Y, Zhao Z, Zhang L, Shen X. Abnormal hypermethylation of promoter region downregulates chemokine CXC ligand 14 expression in gastric cancer. Int J Oncol. 2013; 43: 1487-94. doi: 10.3892/ijo.2013.2078.
18. Cao B, Yang Y, Pan Y, Jia Y, Brock MV, Herman JG, Guo M. Epigenetic silencing of CXCL14 induced colorectal cancer migration and invasion. Discov Med. 2013; 16: 137-47. doi:
19. Sonnet M, Claus R, Becker N, Zucknick M, Petersen J, Lipka DB, Oakes CC, Andrulis M, Lier A, Milsom MD, Witte T, Gu L, Kim-Wanner SZ, et al. Early aberrant

DNA methylation events in a mouse model of acute myeloid leukemia. Genome Med. 2014; 6: 34. doi: 10.1186/gm551.

20. Fotouhi O, Adel Fahmideh M, Kjellman M, Sulaiman L, Hoog A, Zedenius J, Hashemi J, Larsson C. Global hypomethylation and promoter methylation in small intestinal neuroendocrine tumors: An in vivo and in vitro study. Epigenetics. 2014; 9: 987-97. doi: 10.4161/epi.28936.
21. Lin K, Zou R, Lin F, Zheng S, Shen X, Xue X. Expression and effect of CXCL14 in colorectal carcinoma. Mol Med Rep. 2014; 10: 1561-8. doi: 10.3892/mmr.2014.2343.
22. Ellert-Miklaszewska A, Dabrowski M, Lipko M, Sliwa M, Maleszewska M, Kaminska B. Molecular definition of the pro-tumorigenic phenotype of glioma-activated microglia. Glia. 2013; 61: 1178-90. doi: 10.1002/glia.22510.
23. Zeng J, Yang X, Cheng L, Liu R, Lei Y, Dong D, Li F, Lau QC, Deng L, Nice EC, Xie K, Huang C. Chemokine CXCL14 is associated with prognosis in patients with colorectal carcinoma after curative resection. J Transl Med. 2013; 11: 6. doi: 10.1186/1479-5876-11-6.
24. Smallridge RC, Chindris AM, Asmann YW, Casler JD, Serie DJ, Reddi HV, Cradic KW, Rivera M, Grebe SK, Necela BM, Eberhardt NL, Carr JM, McIver B, et al. RNA sequencing identifies multiple fusion transcripts, differentially expressed genes, and reduced expression of immune function genes in BRAF (V600E) mutant vs BRAF wild-type papillary thyroid carcinoma. J Clin Endocrinol Metab. 2014; 99: E338-47. doi: 10.1210/jc.2013-2792.

25. Zhang XH, Wang Q, Gerald W, Hudis CA, Norton L, Smid M, Foekens JA, Massague J. Latent bone metastasis in breast cancer tied to Src-dependent survival signals. Cancer Cell. 2009; 16: 67-78. doi: 10.1016/j.ccr.2009.05.017.
26. Zhang XH, Jin X, Malladi S, Zou Y, Wen YH, Brogi E, Smid M, Foekens JA, Massague J. Selection of bone metastasis seeds by mesenchymal signals in the primary tumor stroma. Cell. 2013; 154: 1060-73. doi: 10.1016/j.cell.2013.07.036.
27. Augsten M, Hagglof C, Olsson E, Stolz C, Tsagozis P, Levchenko T, Frederick MJ, Borg A, Micke P, Egevad L, Ostman A. CXCL14 is an autocrine growth factor for fibroblasts and acts as a multi-modal stimulator of prostate tumor growth. Proc Natl Acad Sci U S A. 2009; 106: 3414-9. doi: 10.1073/pnas.0813144106.
28. Park CR, You DJ, Kim DK, Moon MJ, Lee C, Oh SH, Ahn C, Seong JY, Hwang JI. CXCL14 enhances proliferation and migration of NCI-H460 human lung cancer cells overexpressing the glycoproteins containing heparan sulfate or sialic acid. J Cell Biochem. 2013; 114: 1084-96. doi: 10.1002/jcb.24449.
29. Takiguchi S, Korenaga N, Inoue K, Sugi E, Kataoka Y, Matsusue K, Futagami K, Li YJ, Kukita T, Teramoto N, Iguchi H. Involvement of CXCL14 in osteolytic bone metastasis from lung cancer. Int J Oncol. 2014; 44: 1316-24. doi: 10.3892/ijo.2014.2293.
30. Lu J, Chatterjee M, Schmid H, Beck S, Gawaz M. CXCL14 as an emerging immune and inflammatory modulator. J Inflamm (Lond). 2016; 13: 1. doi: 10.1186/s12950-015-0109-9.
31. Williams KA, Lee M, Hu Y, Andreas J, Patel SJ, Zhang S, Chines P, Elkahloun A, Chandrasekharappa S, Gutkind JS, Molinolo AA, Crawford NP. A systems genetics

approach identifies CXCL14, ITGAX, and LPCAT2 as novel aggressive prostate cancer susceptibility genes. PLoS Genet. 2014; 10: e1004809. doi: 10.1371/journal.pgen.1004809.

32. Zheng X, Carstens JL, Kim J, Scheible M, Kaye J, Sugimoto H, Wu CC, LeBleu VS, Kalluri R. Epithelial-to-mesenchymal transition is dispensable for metastasis but induces chemoresistance in pancreatic cancer. Nature. 2015; 527: 525-30. doi: 10.1038/nature16064.
33. Rothwarf DM, Karin M. The NF-kappa B activation pathway: a paradigm in information transfer from membrane to nucleus. Sci STKE. 1999; 1999: RE1. doi: 10.1126/stke.1999.5.re1.
34. Perkins ND. The diverse and complex roles of NF-kappaB subunits in cancer. Nat Rev Cancer. 2012; 12: 121-32. doi: 10.1038/nrc3204.
35. Yao C, Li P, Song H, Song F, Qu Y, Ma X, Shi R, Wu J. CXCL12/CXCR4 Axis Upregulates Twist to Induce EMT in Human Glioblastoma. Mol Neurobiol. 2016; 53: 3948-53. doi: 10.1007/s12035-015-9340-x.
36. Paraiso KH, Van Der Kooi K, Messina JL, Smalley KS. Measurement of constitutive MAPK and PI3K/AKT signaling activity in human cancer cell lines. Methods Enzymol. 2010; 484: 549-67. doi: 10.1016/B978-0-12-381298-8.00027-7.
37. Ma L, Pei G. Beta-arrestin signaling and regulation of transcription. J Cell Sci. 2007; 120: 213-8. doi: 10.1242/jcs.03338.
38. Coggins NL, Trakimas D, Chang SL, Ehrlich A, Ray P, Luker KE, Linderman JJ, Luker GD. CXCR7 controls competition for recruitment of beta-arrestin 2 in cells

expressing both CXCR4 and CXCR7. PLoS One. 2014; 9: e98328. doi: 10.1371/journal.pone.0098328.

39. Luker KE, Lewin SA, Mihalko LA, Schmidt BT, Winkler JS, Coggins NL, Thomas DG, Luker GD. Scavenging of CXCL12 by CXCR7 promotes tumor growth and metastasis of CXCR4-positive breast cancer cells. Oncogene. 2012; 31: 4750-8. doi: 10.1038/onc.2011.633.
40. Salomonnson E, Stacer AC, Ehrlich A, Luker KE, Luker GD. Imaging CXCL12-CXCR4 signaling in ovarian cancer therapy. PLoS One. 2013; 8: e51500. doi: 10.1371/journal.pone.0051500.
41. Veldkamp CT, Peterson FC, Pelzek AJ, Volkman BF. The monomer-dimer equilibrium of stromal cell-derived factor-1 (CXCL 12) is altered by pH, phosphate, sulfate, and heparin. Protein Sci. 2005; 14: 1071-81. doi: 10.1110/ps.041219505.
42. Ray P, Lewin SA, Mihalko LA, Lesher-Perez SC, Takayama S, Luker KE, Luker GD. Secreted CXCL12 (SDF-1) forms dimers under physiological conditions. Biochem J. 2012; 442: 433-42. doi: 10.1042/BJ20111341.
43. Balabanian K, Lagane B, Infantino S, Chow KY, Harriague J, Moepps B, Arenzana-Seisdedos F, Thelen M, Bachelerie F. The chemokine SDF-1/CXCL12 binds to and signals through the orphan receptor RDC1 in T lymphocytes. J Biol Chem. 2005; 280: 35760-6. doi: 10.1074/jbc.M508234200.
44. Luker KE, Mihalko LA, Schmidt BT, Lewin SA, Ray P, Shcherbo D, Chudakov DM, Luker GD. In vivo imaging of ligand receptor binding with Gaussia luciferase complementation. Nat Med. 2011; 18: 172-7. doi: 10.1038/nm.2590.

45. Chen YC, Allen SG, Ingram PN, Buckanovich R, Merajver SD, Yoon E. Single-cell Migration Chip for Chemotaxis-based Microfluidic Selection of Heterogeneous Cell Populations. Sci Rep. 2015; 5: 9980. doi: 10.1038/srep09980.
46. Schwarze SR, Luo J, Isaacs WB, Jarrard DF. Modulation of CXCL14 (BRAK) expression in prostate cancer. Prostate. 2005; 64: 67-74. doi: 10.1002/pros.20215.
47. Shaykhiev R, Sackrowitz R, Fukui T, Zuo WL, Chao IW, Strulovici-Barel Y, Downey RJ, Crystal RG. Smoking-Induced CXCL14 Expression in the Human Airway Epithelium Links Chronic Obstructive Pulmonary Disease to Lung Cancer. Am J Respir Cell Mol Biol. 2013; 49: 418-25. doi: 10.1165/rcmb.2012-0396OC.
48. Song EY, Shurin MR, Tourkova IL, Gutkin DW, Shurin GV. Epigenetic mechanisms of promigratory chemokine CXCL14 regulation in human prostate cancer cells. Cancer Res. 2010; 70: 4394-401. doi: 10.1158/0008-5472.CAN-10-0427.
49. Greenbaum A, Hsu YM, Day RB, Schuettpelz LG, Christopher MJ, Borgerding JN, Nagasawa T, Link DC. CXCL12 in early mesenchymal progenitors is required for haematopoietic stem-cell maintenance. Nature. 2013; 495: 227-30. doi: 10.1038/nature11926.
50. Aiuti A, Tavian M, Cipponi A, Ficara F, Zappone E, Hoxie J, Peault B, Bordignon C. Expression of CXCR4, the receptor for stromal cell-derived factor-1 on fetal and adult human lympho-hematopoietic progenitors. Eur J Immunol. 1999; 29: 1823-31. doi: 10.1002/(SICI)1521-4141(199906)29:06<1823::AID-IMMU1823>3.0.CO;2-B.
51. Levesque JP, Hendy J, Takamatsu Y, Simmons PJ, Bendall LJ. Disruption of the CXCR4/CXCL12 chemotactic interaction during hematopoietic stem cell

mobilization induced by GCSF or cyclophosphamide. J Clin Invest. 2003; 111: 187-96. doi: 10.1172/JCI15994.

52. Guo Y, Hangoc G, Bian H, Pelus LM, Broxmeyer HE. SDF-1/CXCL12 enhances survival and chemotaxis of murine embryonic stem cells and production of primitive and definitive hematopoietic progenitor cells. Stem Cells. 2005; 23: 1324-32. doi: 10.1634/stemcells.2005-0085.
53. Sharma M, Afrin F, Satija N, Tripathi RP, Gangenahalli GU. Stromal-derived factor-1/CXCR4 signaling: indispensable role in homing and engraftment of hematopoietic stem cells in bone marrow. Stem Cells Dev. 2011; 20: 933-46. doi: 10.1089/scd.2010.0263.
54. Kwok WK, Ling MT, Lee TW, Lau TC, Zhou C, Zhang X, Chua CW, Chan KW, Chan FL, Glackin C, Wong YC, Wang X. Up-regulation of TWIST in prostate cancer and its implication as a therapeutic target. Cancer Res. 2005; 65: 5153-62. doi: 10.1158/0008-5472.CAN-04-3785.
55. Jung Y, Kim JK, Shiozawa Y, Wang J, Mishra A, Joseph J, Berry JE, McGee S, Lee E, Sun H, Wang J, Jin T, Zhang H, et al. Recruitment of mesenchymal stem cells into prostate tumours promotes metastasis. Nat Commun. 2013; 4: 1795. doi: 10.1038/ncomms2766.
56. Li P, Yang R, Gao WQ. Contributions of epithelial-mesenchymal transition and cancer stem cells to the development of castration resistance of prostate cancer. Mol Cancer. 2014; 13: 55. doi: 10.1186/1476-4598-13-55.
57. Uygur B, Wu WS. SLUG promotes prostate cancer cell migration and invasion via CXCR4/CXCL12 axis. Mol Cancer. 2011; 10: 139. doi: 10.1186/1476-4598-10-139.

58. Tanegashima K, Suzuki K, Nakayama Y, Tsuji K, Shigenaga A, Otaka A, Hara T. CXCL14 is a natural inhibitor of the CXCL12-CXCR4 signaling axis. FEBS Lett. 2013; 587: 1731-5. doi: 10.1016/j.febslet.2013.04.046.
59. Otte M, Kliewer A, Schutz D, Reimann C, Schulz S, Stumm R. CXCL14 is no direct modulator of CXCR4. FEBS Lett. 2014; 588: 4769-75. doi: 10.1016/j.febslet.2014.11.009.
60. Collins PJ, McCully ML, Martinez-Munoz L, Santiago C, Wheeldon J, Caucheteux S, Thelen S, Cecchinato V, Laufer JM, Purvanov V, Monneau YR, Lortat-Jacob H, Legler DF, et al. Epithelial chemokine CXCL14 synergizes with CXCL12 via allosteric modulation of CXCR4. FASEB J. 2017. doi: 10.1096/fj.201700013R.
61. Levoye A, Balabanian K, Baleux F, Bachelerie F, Lagane B. CXCR7 heterodimerizes with CXCR4 and regulates CXCL12-mediated G protein signaling. Blood. 2009; 113: 6085-93. doi: 10.1182/blood-2008-12-196618.
62. Decaillot FM, Kazmi MA, Lin Y, Ray-Saha S, Sakmar TP, Sachdev P. CXCR7/CXCR4 heterodimer constitutively recruits beta-arrestin to enhance cell migration. J Biol Chem. 2011; 286: 32188-97. doi: 10.1074/jbc.M111.277038.
63. Steel E, Murray VL, Liu AP. Multiplex detection of homo- and heterodimerization of g protein-coupled receptors by proximity biotinylation. PLoS One. 2014; 9: e93646. doi: 10.1371/journal.pone.0093646.
64. Coke CJ, Scarlett KA, Chetram MA, Jones KJ, Sandifer BJ, Davis AS, Marcus AI, Hinton CV. Simultaneous Activation of Induced Heterodimerization between CXCR4 Chemokine Receptor and Cannabinoid Receptor 2 (CB2) Reveals a

Mechanism for Regulation of Tumor Progression. J Biol Chem. 2016; 291: 9991-10005. doi: 10.1074/jbc.M115.712661.

65. Pello OM, Martinez-Munoz L, Parrillas V, Serrano A, Rodriguez-Frade JM, Toro MJ, Lucas P, Monterrubio M, Martinez AC, Mellado M. Ligand stabilization of CXCR4/delta-opioid receptor heterodimers reveals a mechanism for immune response regulation. Eur J Immunol. 2008; 38: 537-49. doi: 10.1002/eji.200737630.
66. Morrissey C, Roudier MP, Dowell A, True LD, Ketchanji M, Welty C, Corey E, Lange PH, Higano CS, Vessella RL. Effects of androgen deprivation therapy and bisphosphonate treatment on bone in patients with metastatic castration-resistant prostate cancer: results from the University of Washington Rapid Autopsy Series. J Bone Miner Res. 2013; 28: 333-40. doi: 10.1002/jbmr.1749.
67. Xu J, Wang R, Xie ZH, Odero-Marah V, Pathak S, Multani A, Chung LW, Zhau HE. Prostate cancer metastasis: role of the host microenvironment in promoting epithelial to mesenchymal transition and increased bone and adrenal gland metastasis. Prostate. 2006; 66: 1664-73. doi: 10.1002/pros.20488.
68. Allen SG, Chen YC, Madden JM, Fournier CL, Altemus MA, Hiziroglu AB, Cheng YH, Wu ZF, Bao L, Yates JA, Yoon E, Merajver SD. Macrophages Enhance Migration in Inflammatory Breast Cancer Cells via RhoC GTPase Signaling. Sci Rep. 2016; 6: 39190. doi: 10.1038/srep39190.
69. Zhang Z, Chen YC, Cheng YH, Luan Y, Yoon E. Microfluidics 3D gel-island chip for single cell isolation and lineage-dependent drug responses study. Lab Chip. 2016; 16: 2504-12. doi: 10.1039/c6lc00081a.

FIGURE LEGENDS

Figure 1. CXCL14 expression is increased in human PCa bone metastasis. A PCa tissue microarray was immunostained for CXCL14. (**A**) The combined CXCL14 staining H-score was determined. Representative examples of CXCL14 stained samples are shown: normal prostate, benign prostatic hypertrophy (BPH), primary PCa (1° PrCa), lymph node metastasis (LN), soft tissue metastasis (Soft Tiss) and bone metastasis. (**B**) Enlarged magnification of prostate cancer bone metastasis demonstrating intense CXCL14 expression. (**C**) CXCL14 H-score of primary PCa subdivided into Gleason grade. Error bars indicate standard deviation (SD) from the mean. **** $p \leq 0.0001$, NS = not significant.

Figure 2. CXCL14 promoted *in vitro* migration and invasion of human PCa cell lines. (**A**) Representative images from a scratch migration assay using $ARCaP_M$ and PC-3 PCa cells following treatment with CXCL14 (250 ng/ml) or no treatment (NT). (**B**) Invasion assays of $ARCaP_M$ and PC-3 PCa cells were performed using transwell cell culture chambers coated with a cellular matrix. Cancer cells were plated above the membrane and CXCL14 250 ng/ml was present in the bottom chamber. Results are shown after 72 hours of treatment. *** $p \leq 0.001$, NS = not significant, N=3

Figure 3. CXCL14 regulated the expression of genes associated with EMT. RT-PCR was performed to assess TWIST, SNAIL, and SLUG modulation by CXCL14 (10, 100, and 250 ng/ml) in (**A**) $ARCaP_M$ and (**B**) PC-3 cells. After 24 hours of treatment,

RNA was subjected to RT-PCR using specific primers for human *SLUG*, *SNAIL*, and *TWIST*. Messenger RNA concentration was normalized to expression of the *RPL32* housekeeping gene. n=3, * p<0.05, *** p <0.001, **** p <0.0001, NT = no treatment.

Figure 4. CXCL14 increased MAPK and PI3K pathway phosphorylation of PCa cells. (**A**) $ARCaP_M$ and (**B**) PC-3 PCa cells were serum starved for 8 hours. PCa Cells were treated with CXCL14 250 ng/ml and compared to no treatment (NT) for the indicated time (10, 30, 60, and 120 minutes) before cells were lysed. Cell lysates were subjected to western blotting. Lysates were examined for pErk1,2, pAKT, pNF-kB and pSAPK/JNK; total protein corresponding to each phosphoprotein was used as a loading control.

Figure 5. CXCL14 does not recruit β-arrestin 2 to CXCR4. (**A**) MDA-MB-231 cells that stably expressed CXCR4-CBRN/β-arrestin 2-CBC were treated with 50 or 250 ng/ml CXCL14 for 10 minutes then subjected to western blot analysis. Blots were analyzed for phosphorylation of AKT, as a positive control for CXCL14 activity. Bioluminescence assays were performed. Cells were treated with increasing concentrations of CXCL14 alone, CXCL12 alone, or in combination at (**B**) 60 ng/ml and (**C**) 250 ng/ml for one hour. Photon flux values for each time point then were normalized to values obtained for control cells not incubated with chemokine at each time point through 90 min. CXCL12, but not CXCL14, at 60 and 250 ng/ml increased CXCR4/β-arrestin 2 recruitment. The addition of CXCL14 did not alter CXCL12-mediated CXCR4/β-arrestin 2 recruitment. (**D**) The availability of surface CXCR4 after chemokine

treatment was determined. MDA-MB-231 CXCR4-CBRN/β-arrestin 2-CBC cells were treated with CXCL12 or CXCL14 at increasing concentrations for one hour. Then, all groups received 200 ng/ml CXCL12. Bioluminescence was assessed and the peak signal was plotted for each chemokine concentration. CXCL14 pretreatment did not alter CXCL12-mediated recruitment of β-arrestin 2 to CXCR4. However, increasing CXCL12 treatment concentrations reduced β-arrestin 2 recruitment to CXCR4. Data are expressed as mean values ± SEM for fold change relative to control (n=4 per point).

Figure 6. CXCL14 forms a homodimer, but does not interact with CXCR4 or CXCR7. CXCL14 luciferase complementation fusion genes were constructed to investigate the ligand and receptor physical interactions. (**A**) HEK-293T cells were transfected with combinations of CXCL14 or CXCL12, fused to either the LgBit or SmBit of NanoLuc luciferase. Both secreted and cell-associated fractions were tested for bioluminescence. The absolute amount of luminescence was altogether less in the cell-associated compared to the secreted fraction. The inset box is an expanded view of the secreted data from below. Compared to CXCL14 or CXCL12 co-transfected with an irrelevant protein (irrel), CXCL14 and CXCL12 homodimers (homo) were detected in the cell-associated but not the secreted fractions. The existence of a CXCL12/CXCL14 heterodimer (hetero) was detected in the cell-associated fraction. (**B**) HEK-293T cells transfected with CXCL12 or CXCL12 fused to SmBit were co-cultured with equal numbers of cells expressing LgBit-CXCR4 or -CXCR7. As has been previously reported, CXCL12 associated with CXCR4 and CXCR7. A similar interaction was not detected with CXCL14. Graphs show mean values ± SEM for fold change in NanoLuc

luciferase activity relative to background control. **** p ≤ 0.0001; NS = not significant; a = p ≤ 0.0001 compared to CXCL12/irrel hetero and CXCL14/irrel hetero; b = NS compared to CXCL12/irrel hetero and CXCL14/irrel hetero

Figure 7. CXCL14 is dependent on CXCR4 for cellular migration. A microfluidic cell migration assay was utilized to assess the dependence of CXCR4 in CXCL14-mediated cellular migration. For all conditions, four replicates were performed. The breast cancer cell line SUM159 (WT) underwent CXCR4 knockout (KO); KO cells also underwent re-expression of CXCR4 (Add-Back). SUM159 WT, KO, and Add-Back were applied to microfluidic devices with the addition of CXCL14 10 nM (94 ng/ml) at the end of 1000 μm channels. Cells were imaged 24 hours after the addition of CXCL14. Microfluidic devices contained 300 channels and four devices were used for each experimental group. The mean cell migration distance is shown. Significant differences were detected between the CXCL14 WT vs. KO, and KO vs. Add-Back. Data are expressed as mean values ± SD.

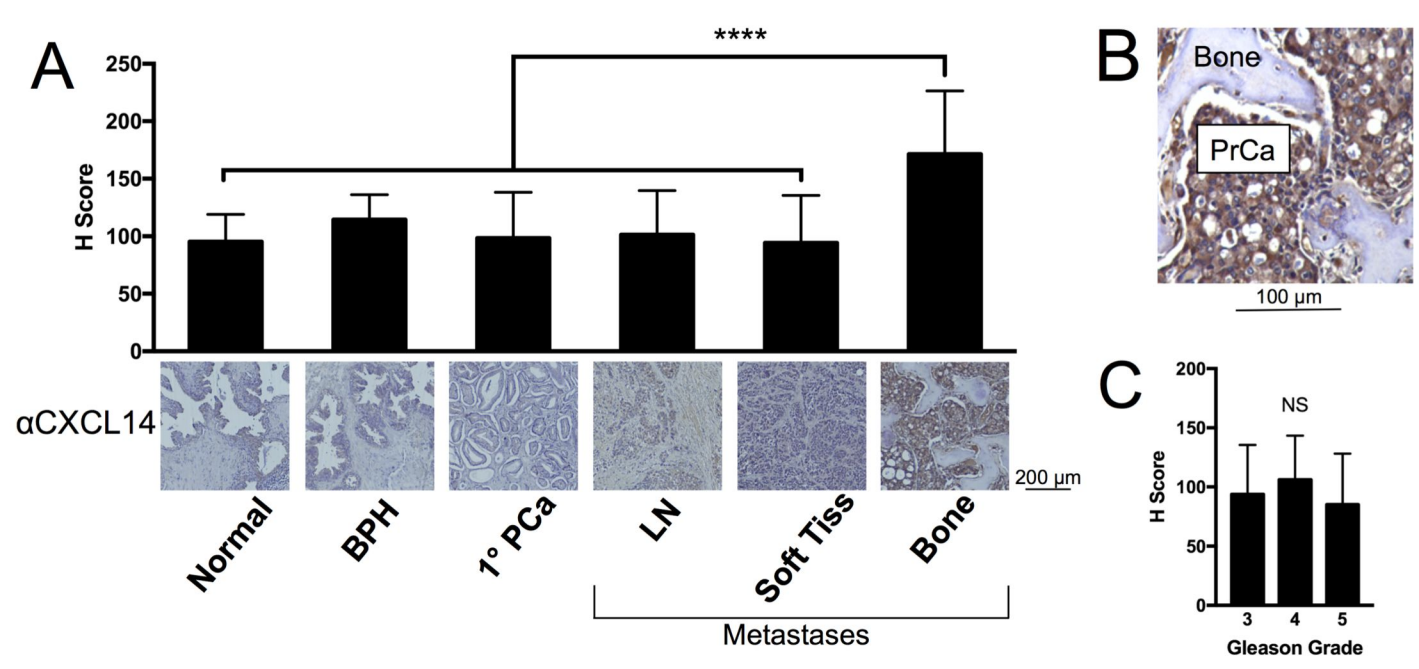
A
****
250
200
150
100
50
0
H Score
αCXCL14
200 µm
Normal
BPH
1° PCa
LN
Soft Tiss
Bone
Metastases
B
Bone
PrCa
100 µm
C
200
150
100
50
0
H Score
NS
3
4
5
Gleason Grade

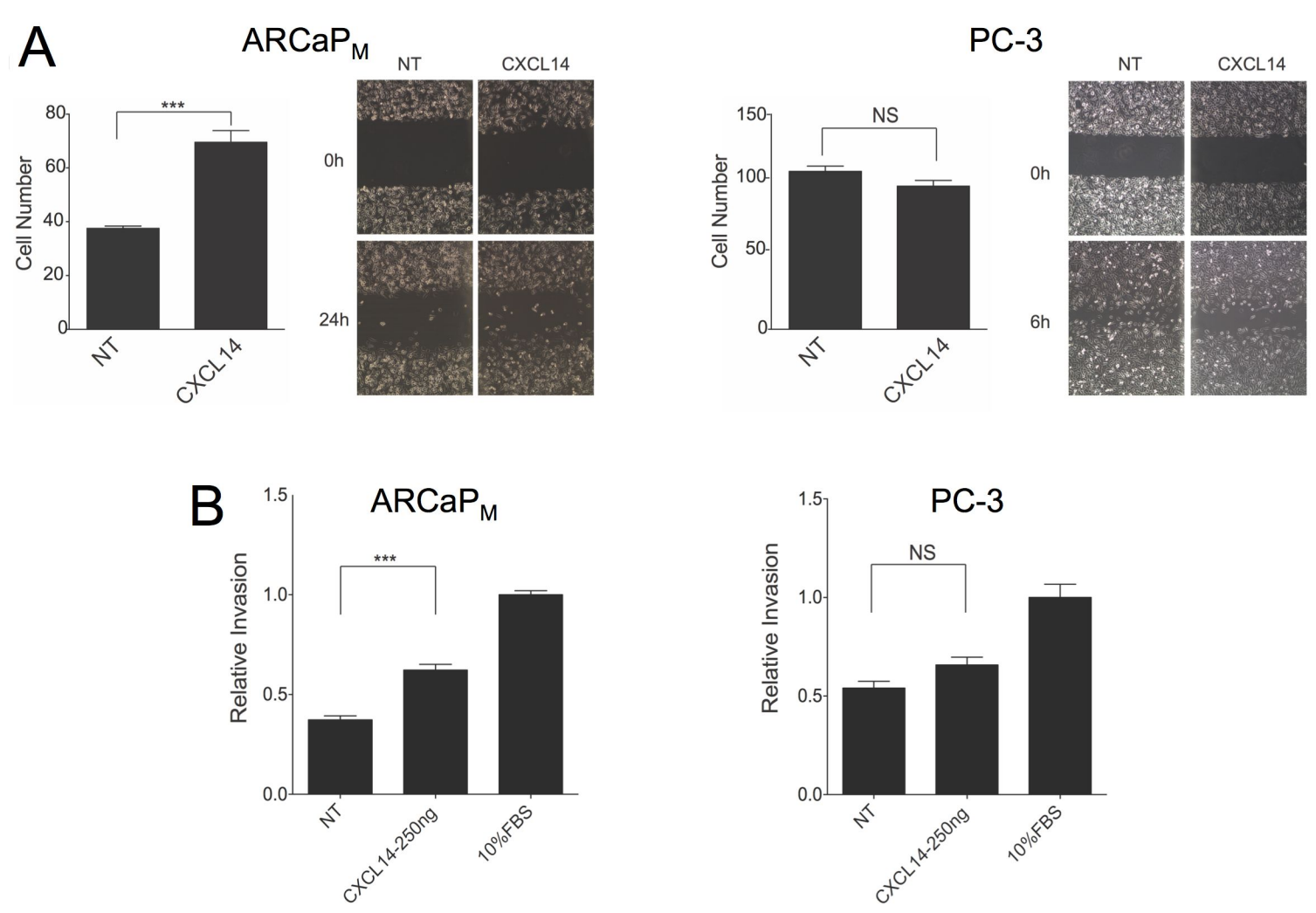
A
ARCaP$_M$
***
Cell Number
80
60
40
20
0
NT
CXCL14
NT
CXCL14
0h
24h
PC-3
NS
150
100
50
0
NT
CXCL14
NT
CXCL14
0h
6h
B
ARCaP$_M$
***
Relative Invasion
1.5
1.0
0.5
0.0
NT
CXCL14-250ng
10%FBS
PC-3
NS
Relative Invasion
1.5
1.0
0.5
0.0
NT
CXCL14-250ng
10%FBS

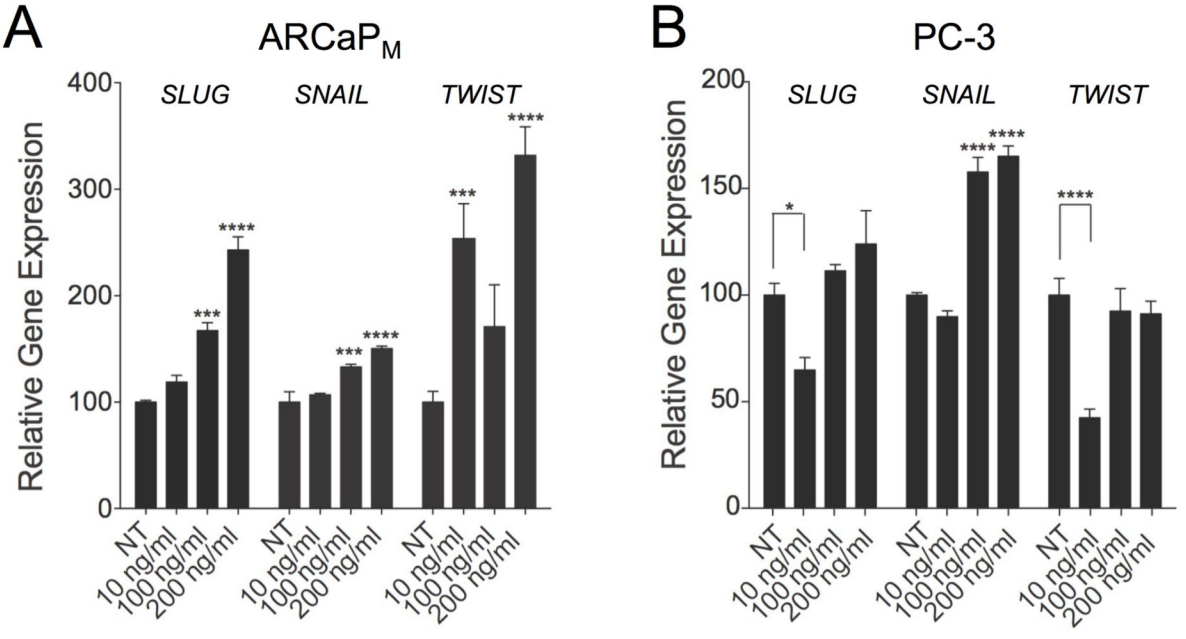
A
ARCaP$_M$
Relative Gene Expression
400
300
200
100
0
SLUG
SNAIL
TWIST
***
****
***
****
***
****
NT
10 ng/ml
100 ng/ml
200 ng/ml
B
PC-3
Relative Gene Expression
200
150
100
50
0
SLUG
SNAIL
TWIST
*
****
****
****
NT
10 ng/ml
100 ng/ml
200 ng/ml

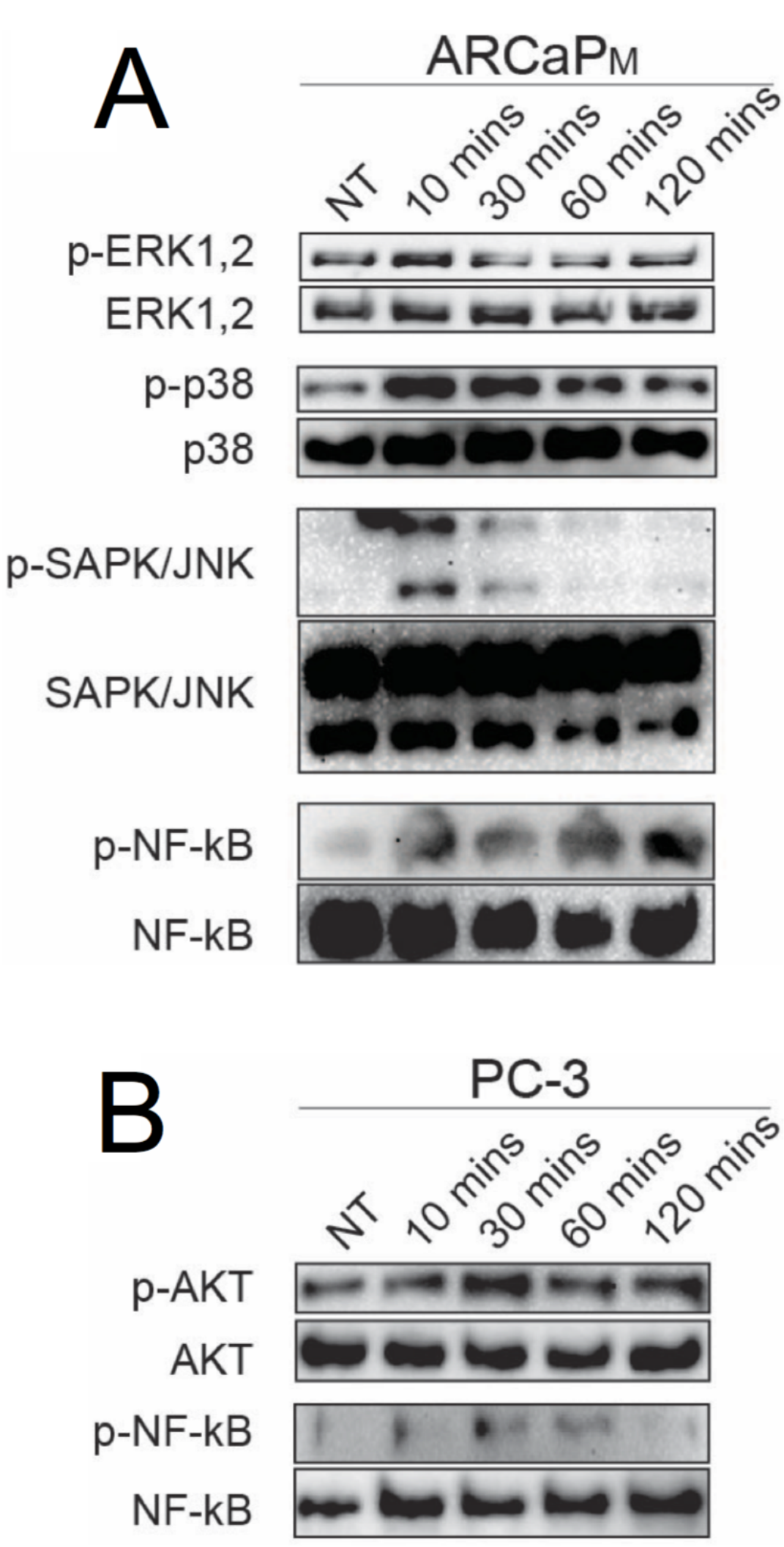
A
ARCaPM
NT
10 mins
30 mins
60 mins
120 mins
p-ERK1,2
ERK1,2
p-p38
p38
p-SAPK/JNK
SAPK/JNK
p-NF-kB
NF-kB
B
PC-3
NT
10 mins
30 mins
60 mins
120 mins
p-AKT
AKT
p-NF-kB
NF-kB

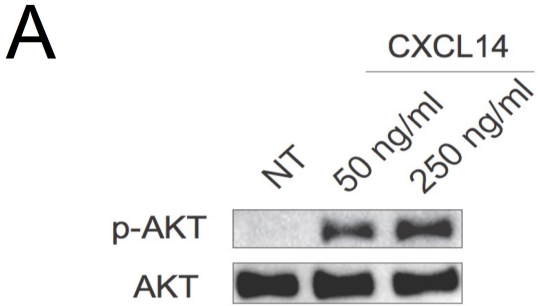
A
CXCL14
NT
50 ng/ml
250 ng/ml
p-AKT
AKT

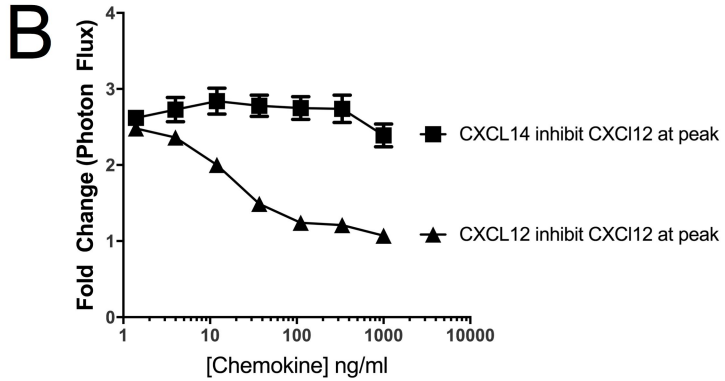
B
Fold Change (Photon Flux)
[Chemokine] ng/ml
CXCL14 inhibit CXCl12 at peak
CXCL12 inhibit CXCl12 at peak

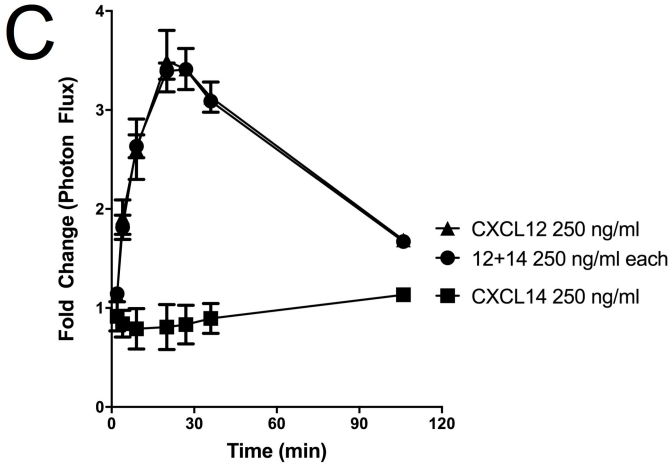
C
Fold Change (Photon Flux)
Time (min)
CXCL12 250 ng/ml
12+14 250 ng/ml each
CXCL14 250 ng/ml

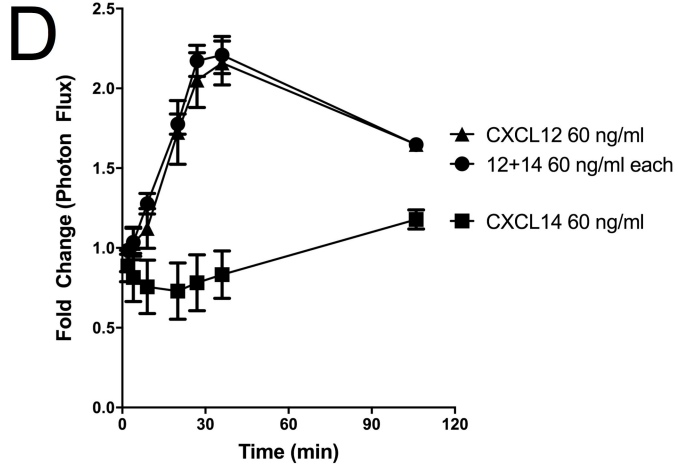
D
Fold Change (Photon Flux)
Time (min)
CXCL12 60 ng/ml
12+14 60 ng/ml each
CXCL14 60 ng/ml

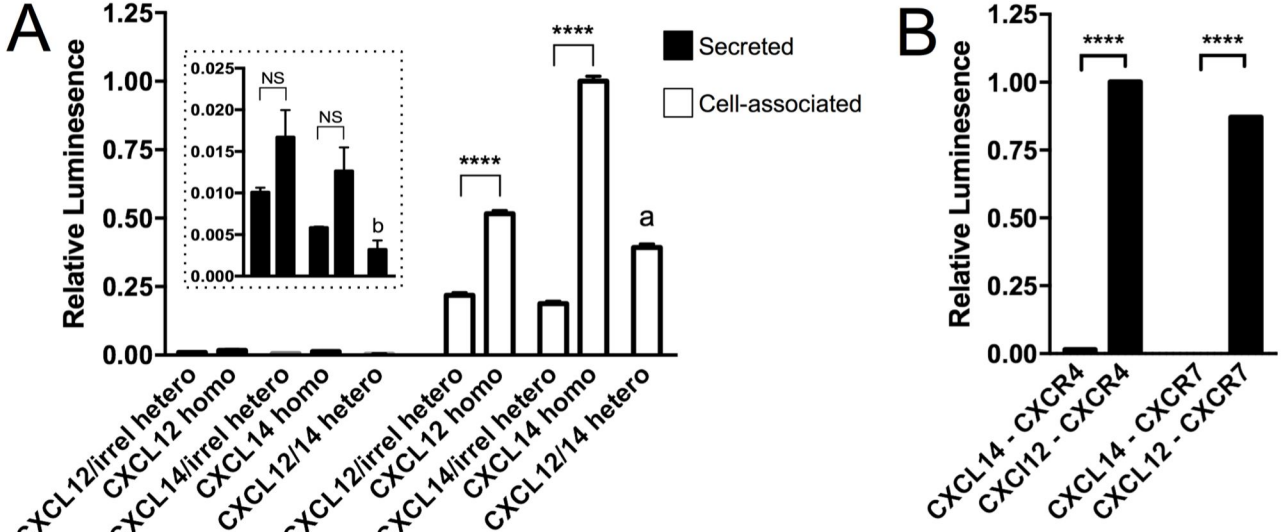
A
Relative Luminesence
1.25
1.00
0.75
0.50
0.25
0.00
0.025
0.020
0.015
0.010
0.005
0.000
NS
NS
b
****
****
a
Secreted
Cell-associated
CXCL12/irrel hetero
CXCL12 homo
CXCL14/irrel hetero
CXCL14 homo
CXCL12/14 hetero
CXCL12/irrel hetero
CXCL12 homo
CXCL14/irrel hetero
CXCL14 homo
CXCL12/14 hetero
B
Relative Luminesence
1.25
1.00
0.75
0.50
0.25
0.00
****
****
CXCL14 - CXCR4
CXCl12 - CXCR4
CXCL14 - CXCR7
CXCL12 - CXCR7

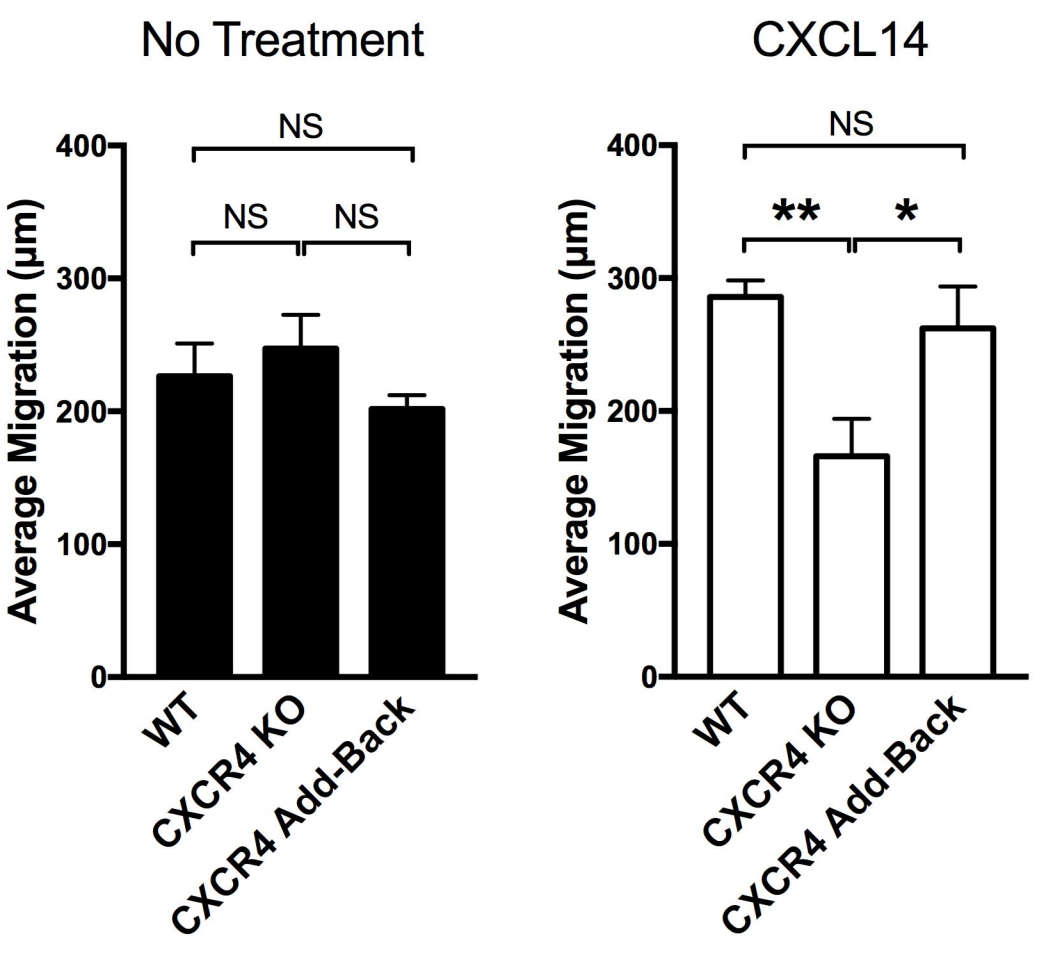
No Treatment
CXCL14
Average Migration (µm)
400
300
200
100
0
NS
NS
NS
**
*
WT
CXCR4 KO
CXCR4 Add-Back